Article

MMS

Mathematics and Mechanics of Solids
2022, Vol. 27(8) 1480–1493

DOI: 10.1177/10812865221094425
journals.sagepub.com/home/mms
SAGE

Elastodynamics of a coated half-space under a sliding contact

V Bratov
Institute for Problems in Mechanical Engineering, Russian Academy of Science, St. Petersburg, Russia; Peter the Great St. Petersburg Polytechnical University, St. Petersburg, Russia

J Kaplunov
School of Computing and Mathematics, Keele University, Keele, UK; Institute for Problems in Mechanical Engineering, Russian Academy of Science, St. Petersburg, Russia

SN Lapatsin
Department of Theoretical and Applied Mechanics, Belarusian State University, Minsk, Belarus

DA Prikazchikov
School of Computing and Mathematics, Keele University, Keele, UK; Institute for Problems in Mechanical Engineering, Russian Academy of Science, St. Petersburg, Russia

Received 9 September 2021; accepted 28 March 2022

Abstract
The paper deals with elastic wave propagating in a layer on a half-space induced by a vertical force. The focus is on the effect of a sliding contact along the interface and its comparative study with a perfect one. The effective boundary conditions substituting the presence of the layer are derived. The leading order term in these conditions corresponds to vertical inertia of the layer, whereas next order correction involves the effect of plate waves in the coating. Analysis of the associated dispersion relation confirms the existence of a Rayleigh-type wave, along with extensional and shear plate waves. An asymptotic hyperbolic-elliptic formulation for surface wave field is also presented. This includes a hyperbolic equation singularly perturbed by a pseudo-differential operator playing a role of a boundary condition for the elliptic equation governing decay over the interior. The sign of the coefficient at the pseudo-differential operator is demonstrated to be always negative, corresponding to a local maximum of the phase speed at zero wave number, and consequently to a distinct receding type of the Rayleigh-type wave quasi-front induced by an impulse load.

Keywords
sliding, asymptotic, thin coating, elastic wave

Corresponding author:
J Kaplunov, School of Computing and Mathematics, Keele University, Keele ST5 5BG, Staffordshire, UK.
Email: j.kaplunov@keele.ac.uk

1. Introduction

Coated structures have various important applications in modern engineering [1–3] to name a few. In spite of numerous publications on the subject, dynamic analysis of such structures is still of substantial interest. Among the robust approximate methods in this area the approach based on derivation of the so-called "effective boundary conditions" along the interface, replacing the effect of a thin coating layer, plays a key role, e.g., see the influential paper by Tiersten [4] and more recent contributions [5,6], and also [7], and references therein. Nowadays, the development of effective boundary conditions usually starts from implementation of the properly adapted asymptotic approach, initially established for thin elastic plates and shells [8–10].

The vast majority of mathematical models for coated structures assume a perfect contact between the coating and the substrate in various scenarios, e.g. see [11–14]. At the same time, only a few papers analyse a sliding contact. For the latter, the full dispersion relation for elastic waves in a layer resting on a half-space was first studied in Achenbach and Keshava [15]. In addition to the dynamic phenomena characteristic of a perfect contact, the presence of an extra longitudinal mode propagating along the coating has been observed. We also mention [16], deriving the effective boundary conditions for a sliding contact by expanding the tractions inside the coating as Taylor series.

The main focus of the publications concerned with elastic linear wave propagation on a coated half-space is usually on Rayleigh-type waves [5,6,17]. In particular, an asymptotic formulation for a long Rayleigh-type wave on a coated half-space for a perfect contact was established in Dai et al. [5]. This paper extends the concept of explicit hyperbolic-elliptic models for surface waves, see the literature [18] and references therein. More recent developments take into account anisotropy and pre-stress [19–21], higher order effects [22], Dirichlet boundary conditions along the surface of a coated half-space [23], the effects of surface oscillators [24, 25], and also include composite plate models [26].

In this paper, we extend the asymptotic methodology in Dai et al. [5] to the case of a sliding contact. Two milestones are crucial for the consideration below. First, we derive effective boundary conditions taking into account a weak coupling between the plane-stress motion of coating with the substrate. These conditions are employed in qualitative dispersion analysis of the problem. We concentrate on the long-wave behaviour of the Rayleigh-type wave, and extra extensional and shear plate waves propagating in the layer. Second, we adapt the derived conditions for formulating an asymptotic model for the surface wave, resulting in a singularly perturbed hyperbolic equation on the interface, as in Dai et al. [5]. Peculiarities of wave phenomena governed by this equation are also addressed.

The paper is organised as follows. As a preliminary, we present an illustative numerical example of a single layer subject to a prescribed transient load at its upper face, and either fixed lower face or the latter under a sliding contact with a rigid base. Comparison of mid-plane displacements performed using finite element software shows that for a sliding contact the tangential displacement significantly dominates over the vertical one, whereas for a fixed lower face both displacements seem to be of the same order. This is in line with initial physical insight, as well as observations of an extra longitudinal mode in Achenbach and Keshava [15], and also more recent findings reported for an elastic contact in Erbaş et al. [27,28].

Then, we derive the effective boundary conditions at the coating/substrate interface using a traditional asymptotic procedure. At leading order, these conditions can be interpreted as the effect of distributed surface vertical inertia. At next order, in contrast to a perfect contact, they support plate wave motion in the coating governed by plane-stress theory.

Next, the associated leading order dispersion relation is analysed within both plane-strain and anti-plane setups. In plane-strain case, a Rayleigh-type wave and an additional extensional "plate" wave are observed, with the phase speed achieving its maximum value equal to the classical Rayleigh wave speed at zero wave number. As might be expected, the anti-plane setup supports only a non-dispersive shear wave on the coating.

Finally, a 3D hyperbolic-elliptic formulation for the Rayleigh-type wave field induced by an arbitrary vertical load is obtained. It is comprised of an elliptic equation for the longitudinal wave potential over the interior of the substrate, and a hyperbolic equation singularly perturbed by a pseudo-differential operator, serving as a boundary condition for the elliptic equation. The presented results are formally similar to those earlier reported in Dai et al. [5] for a perfect contact. However, the coefficient at the pseudo-differential term now takes a simpler form than that in Dai et al. [5] and is shown to be always

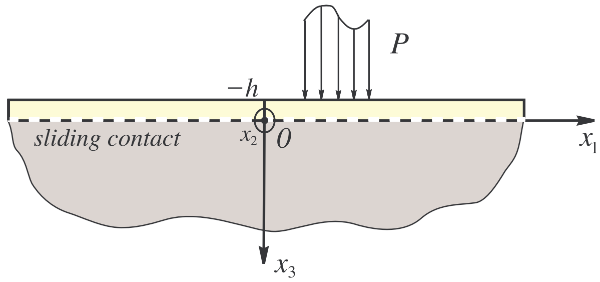

Figure 1. Coated half-space with sliding contact.

negative, whereas the analogous coefficient in Dai et al. [5] changes its sign depending on problem parameters.

2. Statement of the problem

Consider a linearly isotropic, elastic half-space, coated with a thin layer of thickness h, subject to a prescribed vertical force P (Figure 1).

The equations of motion are written conventionally as (see [29]):

$$\operatorname{div} \boldsymbol{\sigma} = \rho_q \frac{\partial^2 \mathbf{u}}{\partial t^2}, \tag{1}$$

where s is the stress tensor, $\mathbf{u} = (u_1, u_2, u_3)$ is the displacement vector, ρ_q is the volume mass density, and index q takes the values $q = c$ and $q = s$, associated with coating and substrate, respectively. The boundary conditions at the surface $x_3 = -h$ are taken in the form:

$$\sigma_{3i} = 0, \quad \sigma_{33} = -P, \tag{2}$$

where $i = 1, 2$, and $P = P(x_1, x_2, t)$ is a prescribed load. On the interface $x_3 = 0$, we assume continuity of vertical displacements and normal tractions, as well as zero tangential stresses, i.e.

$$\sigma_{3i} = [\sigma_{33}] = [u_3] = 0, \tag{3}$$

with $[f] = \lim\limits_{x_3 \to +0} f - \lim\limits_{x_3 \to -0} f$. Here, and further, we mean by the sliding contact a setup in which the tangential stresses along both sides of the interface are equal to zero, see equation (3).

Hooke's law is now adopted in the form convenient for the asymptotic procedure of the next section [8,9]:

$$\begin{aligned}
\sigma_{ij} &= \frac{E_q}{2(1+\nu_q)} \left(\frac{\partial u_i}{\partial x_j} + \frac{\partial u_j}{\partial x_i} \right) \\
\sigma_{3i} &= \frac{E_q}{2(1+\nu_q)} \left(\frac{\partial u_i}{\partial x_3} + \frac{\partial u_3}{\partial x_i} \right) \\
\sigma_{ii} &= \frac{E_q}{1+\nu_q} \left(2\left(1-\kappa_q^2\right) \frac{\partial u_i}{\partial x_i} + \left(1-2\kappa_q^2\right) \frac{\partial u_j}{\partial x_j} \right) + \left(1-2\kappa_q^2\right)\sigma_{33} \\
\frac{\partial u_3}{\partial x_3} &= \frac{1+\nu_q}{E_q} \left(\frac{2\left(1-\kappa_q^2\right)}{3-4\kappa_q^2} \sigma_{33} - \frac{1-2\kappa_q^2}{3-4\kappa_q^2} (\sigma_{11}+\sigma_{22}) \right),
\end{aligned} \tag{4}$$

where $i \neq j = 1, 2$, E_q, and ν_q are Young's moduli and Poisson's ratios, and, as above, $q = c, s$ correspond to either coating or substrate, with,

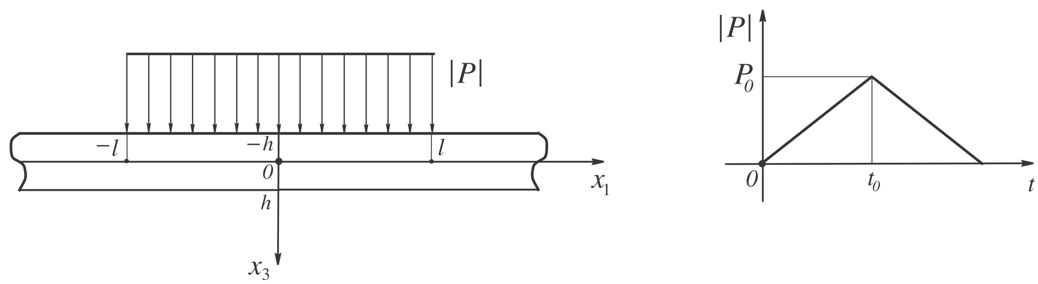

Figure 2. A layer subject to transient load.

$$\kappa_q = \frac{c_{2q}}{c_{1q}} = \sqrt{\frac{1-2\nu_q}{2-2\nu_q}}, \qquad c_{1q} = \sqrt{\frac{E_q \nu_q}{\rho(1+\nu_q)(1-2*nu_q)}}, \qquad c_{2q} = \sqrt{\frac{E_q}{2\rho(1+\nu_q)}}, \tag{5}$$

where c_{1q} and c_{2q} denote the longitudinal and shear wave speeds, respectively.

3. Preliminary numerical insight

Let us present a numerical example stimulating further consideration. For simplicity, we adopt a plane-strain assumption.

Consider an infinite, isotropic, elastic layer $-\infty < x_1 < \infty$, $-h \leqslant x_3 \leqslant h$, under action of a transient vertical load $P = P(x_1, t)$ of the form:

$$P = P_0\,(H(x_1 - l) - H(x_1 + l))\left(1 - |\frac{t}{t_0} - 1|\right), \tag{6}$$

applied over a region $-l \leqslant x_1 \leqslant l$ at the upper face $x_3 = -h$, see Figure 2, showing both the spatial and temporal variation of the load. Here, P_0 is the maximal amplitude of the load, and $2t_0$ is the duration of loading.

In the computations below, the lengths are $h = 0.125$m, $l = 10h$, ensuring the length scale of the load is much greater than the thickness. We also take $t_0 = 0.04$ s and $P_0 = 8$ kN/m. The material properties are chosen as follows: Young's modulus $E = 15$ MPa, Poisson's ratio $\nu = 0.3$, and volume mass density $\rho = 1600$ kg/m^3.

Thus, the boundary conditions on the upper face $x_3 = -h$ are given by:

$$\sigma_{31} = 0, \qquad \sigma_{33} = -P, \tag{7}$$

On the lower face $x = h$, two following scenarios will be compared: either having this face fixed:

$$u_1 = u_3 = 0, \tag{8}$$

or imposing mixed boundary conditions (modelling a sliding contact):

$$u_3 = \sigma_{31} = 0, \tag{9}$$

The horizontal and vertical mid-plane displacements (at $x_3 = 0$) taken at the time instant $t = 0.2$ s are presented for a fixed face (Figure 3) and for a sliding contact (Figure 4).

For fixed lower face (8), see Figure 3, both mid-plane displacements are roughly of the same order $\sim 10^{-7}$. On the contrary, in Figure 4 corresponding to conditions of a sliding contact (9), the horizontal displacement (which is $\sim 10^{-4}$) clearly dominates over the vertical one ($\sim 10^{-6}$).

This simple numerical experiment, performed in LS-DYNA commercial FEM software, already provides a useful preliminary insight, suggesting existence of an extra longitudinal mode, with the dominance of horizontal displacement, supported by mixed boundary conditions. This feature has been recently noted in Erbaş et al. [27] for elastic contact.

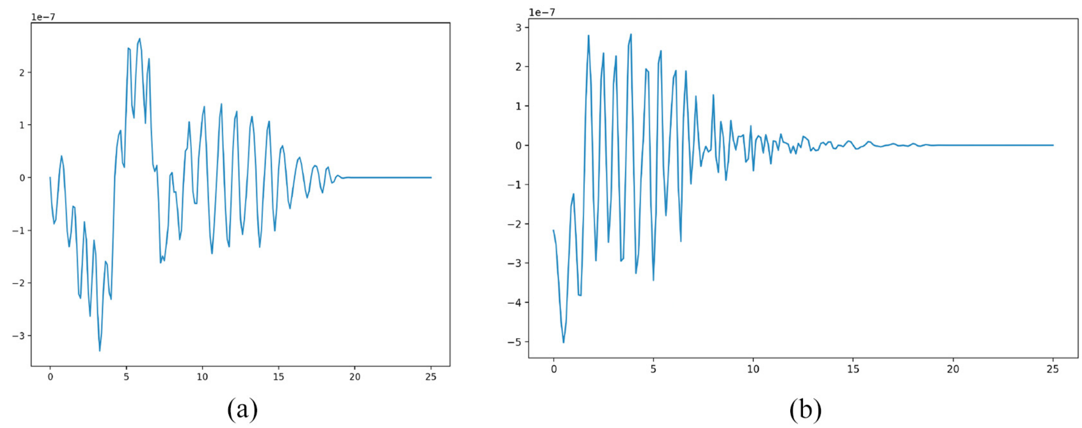

Figure 3. Variations of (a) horizontal and (b) vertical mid-plane displacement along the longitudinal coordinate (fixed lower face $x_3 = h$).

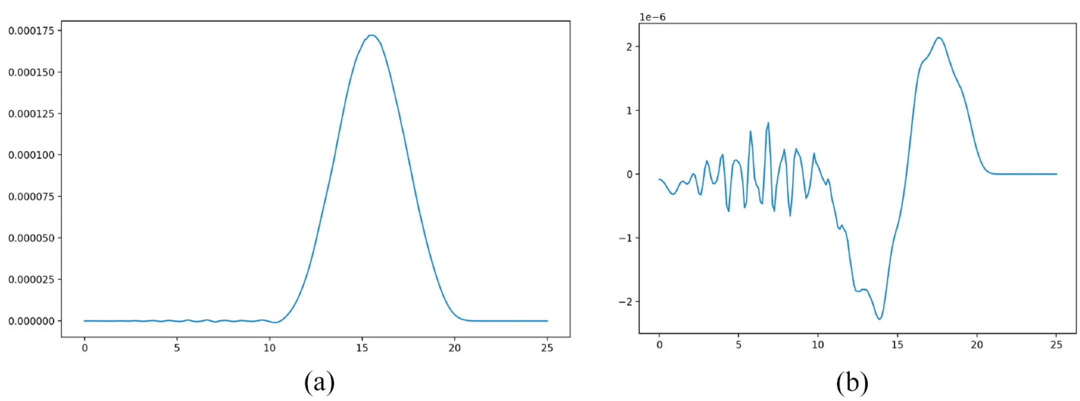

Figure 4. Variations of (a) horizontal and (b) vertical mid-plane displacement along the longitudinal coordinate (sliding contact at $x_3 = -h$).

4. Effective boundary conditions

Let us now derive the effective boundary conditions, modelling the effect of the coating, by means of a long-wave asymptotic procedure [5]. Let us focus on the thin layer first. The equations of motion are given by equation (1), with boundary conditions on the upper face $x_3 = -h$ specified as equation (2), and conditions at the lower face $x_3 = 0$ following from equation (3) as:

$$\sigma_{13} = \sigma_{23} = 0, \quad \sigma_{i3} = 0, \quad u_3 = v_3, \tag{10}$$

where $v_3 = v_3(x_1, x_2, t)$ is the vertical displacement of the substrate at the interface $x_3 = 0$.

Now, to establish an asymptotic procedure, a small parameter associated with the long-wave limit is introduced:

$$\varepsilon = \frac{h}{L} \ll 1, \tag{11}$$

where L is a typical wavelength. Also, the variables and quantities are scaled as:

$$
\begin{aligned}
&\xi_i = \frac{x_i}{L}, \quad \eta = \frac{x_3}{h}, \quad \tau = \frac{c_{2c}t}{L} \\
&u_i = hu_i^*, \quad u_3 = Lu_3^*, \quad v_3 = Lv_3^*, \\
&\sigma_{ii} = \frac{E_c}{2(1+\nu_c)}\,\varepsilon\sigma_{ii}^*, \quad \sigma_{33} = \frac{E_c}{2(1+\nu_c)}\,\varepsilon\sigma_{33}^*, \\
&\sigma_{3i} = \frac{E_c}{2(1+\nu_c)}\,\varepsilon^2\sigma_{3i}^*, \quad \sigma_{12} = \frac{E_c}{2(1+\nu_c)}\,\varepsilon\sigma_{12}^*, \quad P = \frac{E_c}{2(1+\nu_c)}\,\varepsilon P^*,
\end{aligned}
\tag{12}
$$

where $i = 1, 2$, and quantities with the asterisk are assumed to be of the same asymptotic order.

The governing equations for the layer can now be summarised as:

$$
\begin{aligned}
&\frac{\partial\sigma_{ii}^*}{\partial\xi_i} + \frac{\partial\sigma_{ij}^*}{\partial\xi_j} + \frac{\partial\sigma_{3i}^*}{\partial\eta} = \frac{\partial^2 u_i^*}{\partial t^2} \\
&\varepsilon^2\left(\frac{\partial\sigma_{3i}^*}{\partial\xi_i} + \frac{\partial\sigma_{3j}^*}{\partial\xi_j}\right) + \frac{\partial\sigma_{33}^*}{\partial\eta} = \frac{\partial^2 u_3^*}{\partial t^2},
\end{aligned}
\tag{13}
$$

along with the constitutive relations:

$$
\begin{aligned}
&\sigma_{ii}^* = 4\left(1-\kappa_c^2\right)\frac{\partial u_i^*}{\partial\xi_i} + 2\left(1-2\kappa_c^2\right)\frac{\partial u_j^*}{\partial\xi_j} + \left(1-2\kappa_c^2\right)\sigma_{33}^* \\
&\frac{\partial u_3^*}{\partial\eta} = \varepsilon^2\left(\frac{1-\kappa_c^2}{3-4\kappa_c^2}\sigma_{33}^* - \frac{1-2\kappa_c^2}{2\left(3-4\kappa_c^2\right)}\left(\sigma_{11}^* + \sigma_{22}^*\right)\right) \\
&\varepsilon^2\sigma_{3i}^* = \frac{\partial u_3^*}{\partial\xi_i} + \frac{\partial u_i^*}{\partial\eta} \\
&\sigma_{ij}^* = \frac{\partial u_i^*}{\partial\xi_j} + \frac{\partial u_j^*}{\partial\xi_i},
\end{aligned}
\tag{14}
$$

subject to boundary conditions:

$$
\begin{aligned}
&\sigma_{3i}^* = 0, \quad \sigma_{33}^* = -P^*, \quad at \quad \eta = -1 \\
&\sigma_{3i}^* = 0, \quad u_3^* = v_3^*, \quad at \quad \eta = 0,
\end{aligned}
\tag{15}
$$

where, as above, $i \neq j = 1, 2$. The displacements and stresses are now expanded as asymptotic series:

$$
\begin{pmatrix} u_m^* \\ \sigma_{mn}^* \end{pmatrix} = \begin{pmatrix} u_m^{(0)} \\ \sigma_{mn}^{(0)} \end{pmatrix} + \varepsilon^2 \begin{pmatrix} u_m^{(1)} \\ \sigma_{mn}^{(1)} \end{pmatrix} + \ldots, \qquad m, n = 1, 2, 3
\tag{16}
$$

The leading order problem is given by:

$$
\begin{aligned}
&\frac{\partial\sigma_{ii}^{(0)}}{\partial\xi_i} + \frac{\partial\sigma_{ij}^{(0)}}{\partial\xi_j} + \frac{\partial\sigma_{3i}^{(0)}}{\partial\eta} = \frac{\partial^2 u_i^{(0)}}{\partial t^2} \\
&\frac{\partial\sigma_{33}^{(0)}}{\partial\eta} = \frac{\partial^2 u_3^{(0)}}{\partial t^2} \\
&\sigma_{ii}^{(0)} = 4\left(1-\kappa_c^2\right)\frac{\partial u_i^{(0)}}{\partial\xi_i} + 2\left(1-2\kappa_c^2\right)\frac{\partial u_j^{(0)}}{\partial\xi_j} + \left(1-2\kappa_c^2\right)\sigma_{33}^{(0)}
\end{aligned}
\tag{17}
$$

$$\frac{\partial u_3^{(0)}}{\partial \eta} = 0$$
$$\frac{\partial u_3^{(0)}}{\partial \xi_i} + \frac{\partial u_i^{(0)}}{\partial \eta} = 0$$
$$\sigma_{ij}^{(0)} = \frac{\partial u_i^{(0)}}{\partial \xi_j} + \frac{\partial u_j^{(0)}}{\partial \xi_i},$$

subject to:

$$\begin{aligned} &\sigma_{3i}^{(0)} = 0, \quad \sigma_{33}^{(0)} = -P^*, \quad at \quad \eta = -1 \\ &\sigma_{3i}^{(0)} = 0, \quad u_3^{(0)} = v_3^*, \quad at \quad \eta = 0, \end{aligned} \tag{18}$$

The leading order solutions may be found in the form:

$$\begin{aligned} u_i^{(0)} &= -\eta \frac{\partial v_3^*}{\partial \xi_i} + W_i \\ u_3^{(0)} &= v_3^* \\ \sigma_{ii}^{(0)} &= \eta \left(\left(1 - 2\kappa_c^2\right) \left(\frac{\partial^2 v_3^*}{\partial \tau^2} - 2 \frac{\partial^2 v_3^*}{\partial \xi_j^2} \right) - 4\left(1 - \kappa_c^2\right) \frac{\partial^2 v_3^*}{\partial \xi_i^2} \right) \\ &\quad + \left(1 - 2\kappa_c^2\right) \left(\frac{\partial^2 v^*}{\partial \tau^2} + 2 \frac{\partial W_j}{\partial \xi_j} - P^* \right) + 4\left(1 - \kappa_c^2\right) \frac{\partial W_i}{\partial \xi_i} \\ \sigma_{33}^{(0)} &= (\eta + 1) \frac{\partial^2 v_3^*}{\partial \tau^2} - P^* \\ \sigma_{ij}^{(0)} &= -2\eta \frac{\partial^2 v_3^*}{\partial \xi_i \partial \xi_j} + \frac{\partial W_i}{\partial \xi_j} + \frac{\partial W_j}{\partial \xi_i} \\ \sigma_{3i}^{(0)} &= \left(\eta^2 + \eta\right)\left(1 - 2\kappa_c^2\right) \frac{\partial}{\partial \xi_i} \left(2\Delta_\xi v_3^* - \frac{\partial^2 v_3^*}{\partial \tau^2} \right), \end{aligned} \tag{19}$$

where $\Delta_\xi = \frac{\partial^2}{\partial \xi_i^2} + \frac{\partial^2}{\partial \xi_j^2}$ is the 2D Laplacian in ξ_1 and ξ_2, the indices $i \neq j = 1, 2$, and

$$\mathbf{W}(\xi_1, \xi_2, \tau) = (W_1, W_2) = \left(u_1^{(0)}, u_2^{(0)}\right)\big|_{\eta=0}, \tag{20}$$

is a 2D vector of tangential displacements of the layer at the interface $\eta = 0$, satisfying the equation:

$$\begin{aligned} &\frac{\partial^2 \mathbf{W}}{\partial \tau^2} - \Delta_\xi \mathbf{W} - \left(3 - 4\kappa_c^2\right) \mathrm{grad}_\xi \mathrm{div}_\xi \mathbf{W} \\ &\qquad = \mathrm{grad}_\xi \left(2\left(1 - \kappa_c^2\right) \Delta_\xi v_3^* - \frac{\partial^2 v_3^*}{\partial \tau^2} - \left(1 - 2\kappa_c^2\right) P^* \right), \end{aligned} \tag{21}$$

following from the sliding contact conditions at the interface $\eta = 0$. Here, $grad_\xi$ and div_ξ are the gradient and divergence differential operators in ξ_1 and ξ_2.

At next order, we focus our attention on the correction to the normal stress and a related correction to vertical displacement. For these, we have:

$$\frac{\partial u_3^{(1)}}{\partial \eta} = \frac{1-\kappa_c^2}{3-4\kappa_c^2}\sigma_{33}^{(0)} - \frac{1-2\kappa_c^2}{2\left(3-4\kappa_c^2\right)}\left(\sigma_{11}^{(0)}+\sigma_{22}^{(0)}\right)$$
$$\frac{\partial \sigma_{3i}^{(0)}}{\partial \xi_i} + \frac{\partial \sigma_{3j}^{(0)}}{\partial \xi_j} + \frac{\partial \sigma_{33}^{(1)}}{\partial \eta} = \frac{\partial^2 u_3^{(1)}}{\partial t^2}, \tag{22}$$

subject to:

$$\sigma_{33}^{(1)} = 0, \quad at \quad \eta = -1$$
$$u_3^{(1)} = 0, \quad at \quad \eta = 0, \tag{23}$$

The corrector for vertical displacement, satisfying (22, 23) may be written as:

$$u_3^{(1)} = \left(\frac{\eta^2}{2}+\eta\right)\kappa_c^2\frac{\partial^2 v_3^*}{\partial \tau^2} + \frac{\eta^2}{2}\left(1-2\kappa_c^2\right)\Delta_\xi v_3^* - \eta\left(1-2\kappa_c^2\right)\mathrm{div}_\xi \mathbf{W} - \kappa_c^2 P^*, \tag{24}$$

implying the corrector for the normal stress in the form:

$$\sigma_{33}^{(1)} = \frac{\eta^3+1}{6}\left(\kappa_c^2\frac{\partial^4 v_3^*}{\partial \tau^4} + \left(3-4\kappa_c^2\right)\Delta_\xi\frac{\partial^2 v_3^*}{\partial \tau^2} - 4\left(1-\kappa_c^2\right)\Delta_\xi^2 v_3^*\right)$$
$$+ \frac{\eta^2-1}{2}\left(\kappa_c^2\frac{\partial^4 v_3^*}{\partial \tau^4} + (1-\kappa_c^2)\Delta_\xi\left\{\frac{\partial^2 v_3^*}{\partial \tau^2} - 2\Delta_\xi v_3^*\right\} - \left(1-2\kappa_c^2\right)\mathrm{div}_\xi\frac{\partial^2 \mathbf{W}}{\partial \tau^2} - \kappa_c^2\frac{\partial^2 P^*}{\partial \tau^2}\right), \tag{25}$$

Thus, the two-term normal stress on the interface $\eta = 0$ is:

$$\sigma_{33}^* = \frac{\partial^2 v_3^*}{\partial \tau^2} - P^* + \varepsilon^2\left(\frac{1}{3}\left(1-\kappa_c^2\right)\Delta_\xi^2 v_3^* - \frac{1}{6}\kappa_c^2\Delta_\xi\frac{\partial^2 v_3^*}{\partial \tau^2} - \frac{1}{3}\kappa_c^2\frac{\partial^4 v_3^*}{\partial \tau^4}\right.$$
$$\left. + \frac{1}{2}\left(1-2\kappa_c^2\right)\mathrm{div}_\xi\frac{\partial^2 \mathbf{W}}{\partial \tau^2} + \frac{1}{2}\kappa_c^2\frac{\partial^2 P^*}{\partial \tau^2}\right). \tag{26}$$

Returning to the original variables, (26) becomes:

$$\sigma_{33} = \rho_c h\frac{\partial^2 v_3}{\partial t^2} - P + \frac{\rho_c h^3}{6}\left(2c_{2c}^2\left(1-\kappa_c^2\right)\Delta^2 v_3 - \kappa_c^2\Delta\frac{\partial^2 v_3}{\partial t^2} - 2c_{1c}^{-2}\frac{\partial^4 v_3}{\partial t^4}\right)$$
$$+ \frac{h^2}{2}\left(\left(1-2\kappa_c^2\right)\rho_c\,\mathrm{div}\frac{\partial^2 \mathbf{w}}{\partial t^2} + c_{1c}^{-2}\frac{\partial^2 P}{\partial t^2}\right), \tag{27}$$

where $\Delta = \frac{\partial^2}{\partial x_1^2} + \frac{\partial^2}{\partial x_2^2}$ is the 2D Laplacian in x_1 and x_2, and $\mathbf{w}$ is a 2D vector of dimensional tangential displacements of the layer at the interface $x_3 = 0$:

$$\mathbf{w} = (w_1, w_2) = \lim_{x_3 \to 0-}(u_1, u_2), \tag{28}$$

It is interesting to observe from (27) that at leading order the effective normal stress is basically comprised of the prescribed vertical force and the vertical inertia of the layer.

The condition (21) becomes:

$$c_{2c}^{-2}\frac{\partial^2 \mathbf{w}}{\partial t^2} - \Delta\mathbf{w} - \left(3-4\kappa^2\right)\mathrm{grad\ div}\ \mathbf{w}$$
$$= \mathrm{grad}\left(2\left(1-\kappa^2\right)h\Delta v_3 - hc_{2c}^{-2}\frac{\partial^2 v_3}{\partial t^2} - \left(1-2\kappa^2\right)\rho^{-1}c_{2c}^{-2}P\right), \tag{29}$$

where div and grad are the usual diffential operators in x_1 and x_2.

Thus, it may be deduced that for the considered type of a sliding contact the derivation of effective boundary conditions does not allow a straightforward reduction of problem to that for a half-space compared with an ideal contact. The effective conditions on the interface $x_3 = 0$ include the stresses:

$$\sigma_{33} = \rho_c h \frac{\partial^2 u_3}{\partial t^2} - P + \frac{\rho_c h^3}{6}\left(2c_{2c}^2\left(1-\kappa_c^2\right)\Delta^2 u_3 - \kappa_c^2 \Delta \frac{\partial^2 u_3}{\partial t^2} - 2c_{1c}^{-2}\frac{\partial^4 u_3}{\partial t^4}\right)$$
$$+\frac{h^2}{2}\left(\left(1-2\kappa_c^2\right)\rho_c\, div_x \frac{\partial^2 \mathbf{w}}{\partial t^2} + c_{1c}^{-2}\frac{\partial^2 P}{\partial t^2}\right)$$
$$\sigma_{3i} = 0,$$

along with the additional conditions (29), relating the interfacial tangential displacements of the layer w_1 and w_2 with the vertical displacement of the half-space u_3 and the load P. In fact, these conditions govern plate extension waves, allowed by the sliding contact in contrast to the perfect one.

At leading order, when the condition $(30)_1$ at the interface $x_3 = 0$ reduces to:

$$\sigma_{33} = \rho_c h \frac{\partial^2 u_3}{\partial t^2} - P, \tag{31}$$

the problem may be first solved for the half-space and then relation (29) may be used to obtain the tangential displacements of the layer at the interface. Note that the R.H.S of equation (31) corresponds to vertical inertia, with $\rho_c h$ effectively being a distributed mass, providing a justification of problems with inertial terms in boundary conditions [30].

5. Dispersion relation

Now, once effective boundary conditions modelling the interaction with the thin layer have been derived, we proceed with investigation of dispersion of elastic waves in the half-space. Let us first consider plane-strain problem associated with (x_1, x_3) coordinate plane.

The conventional equations of motion are written in terms of the elastic Lamé potentials ϕ and ψ as:

$$\frac{\partial^2 \phi}{\partial x_1^2} + \frac{\partial^2 \phi}{\partial x_3^2} - c_{1s}^{-2}\frac{\partial^2 \phi}{\partial t^2} = 0, \qquad \frac{\partial^2 \psi}{\partial x_1^2} + \frac{\partial^2 \psi}{\partial x_3^2} - c_{2s}^{-2}\frac{\partial^2 \psi}{\partial t^2} = 0, \tag{32}$$

with the displacements expressed as:

$$u_1 = \frac{\partial \phi}{\partial x_1} - \frac{\partial \psi}{\partial x_3}, \qquad u_3 = \frac{\partial \phi}{\partial x_3} + \frac{\partial \psi}{\partial x_1}, \tag{33}$$

In absence of loading ($P = 0$), the leading order effective boundary conditions at $x_3 = 0$ follow from equations (30) and (29) as:

$$\begin{aligned}\sigma_{33} &= \rho_s c_{2s}^2\left(\left(\kappa_s^{-2}-2\right)\frac{\partial u_1}{\partial x_3} + \kappa_s^{-2}\frac{\partial u_3}{\partial x_3}\right) = \rho_c h \frac{\partial^2 u_3}{\partial t^2}\\ \sigma_{31} &= \rho_s c_{2s}^2\left(\frac{\partial u_1}{\partial x_3} + \frac{\partial u_3}{\partial x_1}\right) = 0,\end{aligned} \tag{34}$$

and

$$c_{2c}^{-2}\frac{\partial^2 w_1}{\partial t^2} - 4\left(1-\kappa_c^2\right)\frac{\partial^2 w_1}{\partial x_1^2} = h\left(2\left(1-\kappa_c^2\right)\frac{\partial^3 u_3}{\partial x_1^3} - c_{2c}^{-2}\frac{\partial^3 u_3}{\partial x_1 \partial t^2}\right), \tag{35}$$

The solutions for the potentials (satisfying the decay conditions at $x_3 \to \infty$) of harmonic exponential profile may be found from equation (32) as:

$$\phi = Ae^{ik(x_1 - ct) - kq_1x_3}, \qquad \psi = Be^{ik(x_1 - ct) - kq_2x_3}, \tag{36}$$

where k is wave number, c is the sought for phase speed, and

$$q_j = \sqrt{1 - \frac{c^2}{c_{js}^2}}, \quad j = 1, 2, \tag{37}$$

implying a similar harmonic profile for the interfacial displacement of the layer:

$$w_1 = We^{ik(x_1 - ct)}, \tag{38}$$

Using equation (33) and substituting the quantities (36) and (38) into the boundary conditions (34), we arrive at a homogeneous algebraic system in A, B, and W. From solvability of the latter, the associated determinant must vanish, leading to the dispersion relation:

$$\left[\rho_s c_{2s}^4\left(4q_1q_2 - \left(1 + q_2^2\right)^2\right) - khq_1\rho_c c^4\right]\left(c_3^2 - c^2\right) = 0, \tag{39}$$

where

$$c_3 = 2c_{2c}\sqrt{1 - \kappa_c^2} = \sqrt{\frac{E_c}{\rho_c\left(1 - \nu_c^2\right)}}, \tag{40}$$

is the so-called "plate" speed, associated with sliding of the layer. A similar observation was made earlier by Achenbach and Keshava [15] when analysing full dispersion relation for the original problem for a coated half-space (cf. equation (32) in the cited paper).

The first term in square brackets in (39) describes dispersion of the Rayleigh-type wave. On introducing the dimensionless wave number K and speed C:

$$K = kh, \qquad C = \frac{c}{c_{2s}}, \tag{41}$$

this relation may be rewritten as:

$$(2 - C^2)^2 - 4\sqrt{1 - C^2}\sqrt{1 - \kappa_s^2 C^2} + \frac{\rho_c}{\rho_s}K\sqrt{1 - \kappa_s^2 C^2}\, C^4 = 0, \tag{42}$$

Clearly, the area of interest is in the long-wave vicinity as $K \to 0$. It is evident from equation (42) that if $K = 0$, this equation coincides with the classical Rayleigh equation (same happens if the density of the layer ρ_c is set to zero):

$$(2 - C^2)^2 - 4\sqrt{1 - C^2}\sqrt{1 - \kappa_s^2 C^2} = 0. \tag{43}$$

A typical dispersion diagram is shown Figure 5, illustrating dependence of the scaled phase speed C on the scaled wave number K for Poisson's ratio $\nu = \frac{1}{4}$ when the densities of the layer and the substrate coincide ($\rho_c = \rho_s$). It may be readily deduced from equation (42) that if $\rho_c \neq \rho_s$, the plot will be obtained from Figure 5 by horizontal compression.

The phase speed C is observed to be a monotonously decaying function of the wave number K, having a maximum at the Rayleigh wave speed $C = C_R$, occurring at $K = 0$. Indeed, the derivative at the long-wave limit $K = 0, C = C_R$ is negative:

$$\frac{dC}{dK}\Big|_{C = C_R} = -\frac{\rho_c}{\rho_s}\frac{q_{1R}C_R^5}{4B} < 0, \tag{44}$$

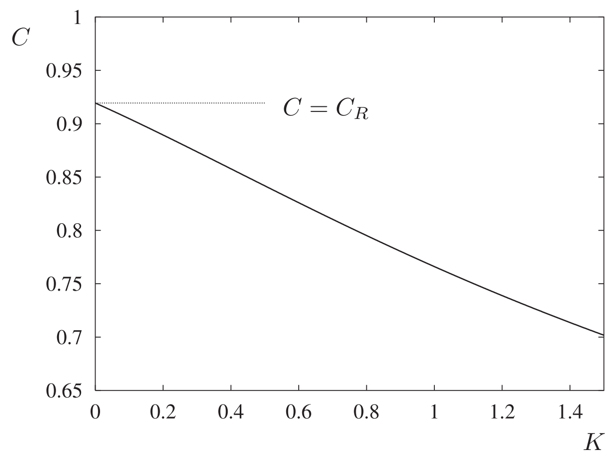

Figure 5. Dispersion curve and the associated long-wave limit $C = C_R$ for $\nu = \frac{1}{4}$ and $\rho_s = \rho_c$.

where

$$q_{1R} = \sqrt{1 - \kappa_s^2 C_R^2}, \qquad B = \frac{q_{1R}}{q_{2R}}\left(1 - q_{2R}^2\right) + \frac{q_{2R}}{q_{1R}}\left(1 - q_{1R}^2\right) - 1 + q_{2R}^4, \qquad q_{2R} = \sqrt{1 - C_R^2}, \tag{45}$$

with constant B, appearing also in the hyperbolic-elliptic model for the Rayleigh wave, see equation (93) in Kaplunov and Prikazchikov [18], known to be positive. Curiously, this implies that for a sliding contact only the scenario of a local maximum at Rayleigh wave speed could be realised, contrary to a perfect contact considered in Dai et al. [5] allowing both local maximum and local minimum.

Now, let us discuss briefly the anti-plane setup, following equations (30) and (29). On assuming $w_1 = u_1 = u_3 = 0$ and $w_2 = w_2(x_1, t)$, $u_2 = u_2(x_1, x_3, t)$, in absence of the load ($P = 0$) we have the classical wave equation of motion for the substrate:

$$\frac{\partial^2 u_2}{\partial x_1^2} + \frac{\partial^2 u_2}{\partial x_3^2} - c_{2s}^{-2}\frac{\partial^2 u_2}{\partial t^2} = 0, \tag{46}$$

subject to conditions at the interface $x_3 = 0$:

$$\begin{aligned} \sigma_{32} = \rho_s c_{2s}^2 \frac{\partial u_2}{\partial x_3} &= 0 \\ c_{2c}^{-2}\frac{\partial^2 w_2}{\partial t^2} - \frac{\partial^2 w_2}{\partial x_1^2} &= 0, \end{aligned} \tag{47}$$

Thus, in anti-plane setup, the shear motions of the layer and substrate are separated completely. The substrate does not support a localised wave, whereas a shear wave is still a feature of the coating.

6. Asymptotic formulation for the Rayleigh-type wave

Let us now present an explicit model for the Rayleigh-type wave induced by a prescribed arbitrary vertical load $P = P(x_1, x_2, t)$. The boundary conditions at the surface $x_3 = 0$ are given by equation (31) and homogeneous conditions on shear surface stresses in equation (30) corresponding to the considered sliding contact:

$$\sigma_{13} = \sigma_{23} = 0, \quad \sigma_{33} = \rho_c h \frac{\partial^2 u_3}{\partial t^2} - P, \tag{48}$$

Then, using the same slow-time perturbation procedure as exposed in Dai et al. [5], see also literature [18] and references therein for more details, we obtain an asymptotic formulation for the near-surface zone. This includes an elliptic equation:

$$\frac{\partial^2 \phi}{\partial x_3^2} + q_{1R}^2 \Delta \phi = 0, \tag{49}$$

for the longitudinal wave potential ϕ, governing the decay over the interior $x_3 > 0$, and a hyperbolic equation singularly perturbed by a pseudo-differential operator given by:

$$\frac{\partial^2 \phi}{\partial x_1^2} - \frac{1}{c_R^2}\frac{\partial^2 \phi}{\partial t^2} + A\sqrt{-\Delta}\Delta\phi = \frac{1+q_{2R}^2}{2\rho_s c_{2s}^2 B} P, \tag{50}$$

along the surface $x_3 = 0$. Here, q_{1R}, q_{2R} and B were defined in equation (45), $c_R = c_{2s} C_R$ is the dimensional Rayleigh wave speed in the substrate, Δ is the 2D Laplace operator in x_1 and x_2, and the constant A is expressed as:

$$A = -\frac{\rho_c}{\rho_s}\frac{C_R^4}{2B} q_{1R} h, \tag{51}$$

In the last formula, it is important that $A < 0$, since all the quantities in the RHS, including B, are positive. The remaining formulae for the vector shear potential and displacement components can be found in Kaplunov and Prikazchikov [18] (see formulae (121) and (122)).

Note that within the plane-strain setup, say for (x_1, x_3) plane the pseudo-differential equation (50) takes the form:

$$\frac{\partial^2 \phi}{\partial x_1^2} - \frac{1}{c_R^2}\frac{\partial^2 \phi}{\partial t^2} + A\sqrt{-\frac{\partial^2}{\partial x_1^2}}\frac{\partial^2 \phi}{\partial x_1^2} = \frac{1+q_{2R}^2}{2\rho_s c_{2s}^2 B} P, \tag{52}$$

Taking into account equation (51), the associated dispersion relation becomes:

$$\frac{\rho_c}{\rho_s}\frac{C_R^4}{2B} q_{1R} K - 1 + \frac{C^2}{C_R^2} = 0, \tag{53}$$

with the dimensionless wave number K and speed C defined in equation (41).

It can be easily verified that the equation (53) provides a long-wave approximation to the dispersion relation (42) and the derivative $\frac{dC}{dK}$ calculated from (53) at the point $K = 0, C = C_R$ coincides with its counterpart in equation (44).

In addition, the local maximum of the phase velocity at zero wave number, see Figure 5, which corresponds to negative sign of coefficient A in pseudo-differential operator (52), determines the type of quasi-front induced by a point impulse when $P = P_0 \delta(x_1)\delta(t)$. Due to similarity of a pseudo-differential equation (52) with that studied in Dai et al. [5] (cf. equation (35) of the cited paper), the analysis of the quasi-front for a sliding contact is virtually the same. However, since $A < 0$ in equation (52), the latter supports only a receding quasi-front, whereas for a perfect contact treated in Dai et al. [5] both receding and advancing quasi-fronts are observed, see Figure 4 in Dai et al. [5].

7. Conclusion

3D dynamic problem in linear elasticity for a thin layer in sliding contact with a half-space subject to a prescribed vertical force has been considered. The effective boundary conditions (29) and (30) accounting for the effect of the coating have been derived. At leading order, these contain only the terms corresponding to the vertical inertia of the coating. At next order, they are also effected by plate waves in the layer governed by 2D plane-stress theory. The observed feature seems to be specific for a sliding contact, in contrast to a perfect contact prohibiting natural vibrations of the coating. As a result, the associated dispersion relation involves not only a Rayleigh-type but also extensional and shear plate waves.

In addition, an explicit hyperbolic-elliptic model for the Rayleigh-type wave is formulated, complementing the previously known formulation for a perfect contact [5]. The presented model is comprised of a hyperbolic equation singularly perturbed by a pseudo-differential operator, serving as a boundary condition for an elliptic equation governing decay over the interior. The coefficient at the pseudo-differential operator is shown to be always negative, corresponding to a local maximum of the phase speed observed at zero wave number. For an impulse loading, this results in a receding quasi-front, whereas a similar problem for a perfect contact [5] allows both positive and negative values of the aforementioned coefficient. Consequently, both maximum/minimum of the phase speed and receding/advancing quasi-fronts may arise at a perfect contact.

The obtained results may find various applications in theory and practice of elastic coatings. For example, delamination and fracture of a perfect contact may be accompanied by excitation of extensional and shear plate waves in the coating, and may possibly change the type of the Rayleigh wave quasi-front. Further developments may also incorporate the effects of curvature, anisotropy, as well as more sophisticated types of contact [31,32].

Funding

The author(s) disclosed receipt of the following financial support for the research, authorship, and/or publication of this article: Support from the Russian Science Foundation (Grant No. 20-11-20133) is gratefully acknowledged.

References

[1] Veprek, S, and Veprek-Heijman, MJ. Industrial applications of superhard nanocomposite coatings. *Surf Coat Technol* 2008; 202(21): 5063–5073.
[2] Hauert, R. A review of modified DLC coatings for biological applications. *Diam Relat Mater* 2003; 12: 583–589.
[3] Ong, G, Kasi, R, and Subramaniam, R. A review on plant extracts as natural additives in coating applications. *Prog Org Coat* 2021; 151: 106091.
[4] Tiersten, HF. Elastic surface waves guided by thin films. *J Appl Phys* 1969; 40(2): 770–789.
[5] Dai, H, Kaplunov, J, and Prikazchikov, D. A long-wave model for the surface elastic wave in a coated half-space. *Proc R Soc* 2010; 466: 3097–3116.
[6] Vinh, PC, and Anh, VTN. Effective boundary condition method and approximate secular equations of Rayleigh waves in orthotropic half-spaces coated by a thin layer. *J Mech Mater Struct* 2016; 11(3): 259–277.
[7] Kaplunov, J, Prikazchikov, D, and Sultanova, L. On higher order effective boundary conditions for a coated elastic half-space. In: Andrianov, I, Manevich, A, Mikhlin, Y, et al. (eds) *Problems of nonlinear mechanics and physics of materials*. Cham: Springer, 2019, pp. 449–462.
[8] Goldenveizer, AL. *Theory of elastic thin shells*. 2nd ed. Moscow: Nauka, 1976.
[9] Kaplunov, JD, Kossovich, LY, and Nolde, EV. *Dynamics of thin walled elastic bodies*. New York: Academic Press, 1998.
[10] Aghalovyan, LA. *Asymptotic theory of anisotropic plates and shells*. Singapore: World Scientific, 2015.
[11] Cai, Z, and Fu, Y. On the imperfection sensitivity of a coated elastic half-space. *Proc R Soc A* 1999; 455: 3285–3309.
[12] Bigoni, D, Gei, M, and Movchan, AB. Dynamics of a prestressed stiff layer on an elastic half space: filtering and band gap characteristics of periodic structural models derived from long-wave asymptotics. *J Mech Phys Solids* 2008; 56(7): 2494–2520.
[13] Liu, Y, and Dai, HH. Compression of a hyperelastic layer-substrate structure: transitions between buckling and surface modes. *Int J Eng Sci* 2014; 80: 74–89.
[14] Tian, R, Nie, G, Liu, J, et al. On Rayleigh waves in a piezoelectric semiconductor thin film over an elastic half-space. *Int J Mech Sci* 2021; 204: 106565.
[15] Achenbach, JD, and Keshava, SP. Free waves in a plate supported by a semi-infinite continuum. *ASME J Appl Mech* 1967; 34: 397–404.
[16] Vinh, PC, Anh, VTN, and Thanh, VP. Rayleigh waves in an isotropic elastic half-space coated by a thin isotropic elastic layer with smooth contact. *Wave Motion* 2014; 51(3): 496–504.
[17] Steigmann, DJ, and Ogden, RW. Surface waves supported by thin-film/substrate interactions. *IMA J Appl Math* 2007; 72(6): 730–747.
[18] Kaplunov, J, and Prikazchikov, D. Asymptotic theory for Rayleigh and Rayleigh-type waves. In: Bordas, SPA, and Balint, DS (eds) *Advances in applied mechanics*. London: Elsevier, 2017, pp. 1–106.

[19] Nobili, A, and Prikazchikov, D. Explicit formulation for the Rayleigh wave field induced by surface stresses in an orthorhombic half-plane. *Eur J Mech A: Solid* 2018; 70: 86–94.
[20] Fu, Y, Kaplunov, J, and Prikazchikov, D. Reduced model for the surface dynamics of a generally anisotropic elastic half-space. *Proc R Soc A* 2020; 476(2234): 20190590.
[21] Khajiyeva, L, Prikazchikov, D, and Prikazchikova, L. Hyperbolic-elliptic model for surface wave in a pre-stressed incompressible elastic half-space. *Mech Res Commun* 2018; 92: 49–53.
[22] Wootton, P, Kaplunov, J, and Prikazchikov, D. A second-order asymptotic model for Rayleigh waves on a linearly elastic half plane. *IMA J Appl Math* 2020; 85(1): 113–131.
[23] Kaplunov, J, Prikazchikov, D, and Sultanova, L. Rayleigh-type waves on a coated elastic half-space with a clamped surface. *Philos Trans R Soc A* 2019; 377(2156): 20190111.
[24] Ege, N, Erbaş, B, Kaplunov, J, et al. Approximate analysis of surface wave-structure interaction. *J Mech Mater Struct* 2018; 13(3): 297–309.
[25] Wootton, P, Kaplunov, J, and Colquitt, D. An asymptotic hyperbolic-elliptic model for flexural-seismic metasurfaces. *Proc R Soc A* 2020; 475(2227): 20190079.
[26] Erbaş, B, Kaplunov, J, Nolde, E, et al. Composite wave models for elastic plates. *Proc R Soc A* 2018; 474(2214): 20180103.
[27] Erbaş, B, Kaplunov, J, Nobili, A, et al. Dispersion of elastic waves in a layer interacting with a Winkler foundation. *J Acoust Soc Am* 2018; 144(5): 2918–2925.
[28] Erbaş, B, Kaplunov, J, and Elishakoff, I. Asymptotic derivation of a refined equation for an elastic beam resting on a Winkler foundation. *Math Mech Solids*. Epub ahead of print 15 June 2021. DOI: 10.1177/10812865211023885.
[29] Achenbach, JD. *Wave propagation in elastic solids*. New York: North Holland, 1973.
[30] Sarkisyan, A, and Sarkisyan, S. Waves in elastic layer with inertial mass on the boundary. *Proc Natl Acad Sci Armen* 2018; 72(1): 65–72.
[31] Borodich, FM, Galanov, BA, Perepelkin, NV, et al. Adhesive contact problems for a thin elastic layer: asymptotic analysis and the JKR theory. *Math Mech Solids* 2019; 24(5): 1405–1424.
[32] Golub, MV, Wilde, M, Eremin, A, et al. The potential of ultrasonic edge and Lamb waves propagating in laminates to detect defects near an edge and weakened adhesion zones. In: Rizzo, P, and Milazzo, A (eds) *European Workshop on Structural Health Monitoring*. Cham: Springer, 2020, pp. 809–818.